# Increase in Endoplasmic Reticulum Stress–Related Proteins and Genes in Adipose Tissue of Obese, Insulin-Resistant Individuals

**Guenther Boden,[1] Xunbao Duan,[2] Carol Homko,[1] Ezequiel J. Molina,[3] WeiWei Song,[1] Oscar Perez,[2] Peter Cheung,[1] and Salim Merali[2]**

**OBJECTIVE**—To examine fat biopsy samples from lean insulin-sensitive and obese insulin-resistant nondiabetic individuals for evidence of endoplasmic reticulum (ER) stress.

**RESEARCH DESIGN AND METHODS**—Subcutaneous fat biopsies were obtained from the upper thighs of six lean and six obese nondiabetic subjects. Fat homogenates were used for proteomic (two-dimensional gel and MALDI-TOF/TOF), Western blot, and RT-PCR analysis.

**RESULTS**—Proteomic analysis revealed 19 differentially upregulated proteins in fat of obese subjects. Three of these proteins were the ER stress–related unfolded protein response (UPR) proteins calreticulin, protein disulfide-isomerase A3, and glutathione-*S*-transferase P. Western blotting revealed upregulation of several other UPR stress–related proteins, including calnexin, a membrane-bound chaperone, and phospho c-jun $NH_2$-terminal kinase (JNK)-1, a downstream effector protein of ER stress. RT-PCR analysis revealed upregulation of the spliced form of X-box binding protein-1s, a potent transcription factor and part of the proximal ER stress sensor inositol-requiring enzyme-1 pathway.

**CONCLUSIONS**—These findings represent the first demonstration of UPR activation in subcutaneous adipose tissue of obese human subjects. As JNK can inhibit insulin action and activate proinflammatory pathways, ER stress activation of JNK may be a link between obesity, insulin resistance, and inflammation. ***Diabetes*** **57:2438–2444, 2008**

Obesity is associated with insulin resistance and with a low-grade state of inflammation (1). Whereas the cause of neither is completely understood, there is good evidence to show that free fatty acids (FFAs) play an important role in the development of obesity-related insulin resistance and inflammation (2). Plasma FFA levels are increased in most obese people (3). Acutely raising plasma FFA levels increases insulin resistance (4), whereas lowering plasma FFA levels reduces insulin resistance (5). Mechanisms involved in FFA-induced insulin resistance include accumulation (in muscle and liver) of lipids and lipid intermediates, including diacylglycerol; activation of several protein kinase C isoforms; and reduction in tyrosine phosphorylation of insulin receptor substrate-1/2 (6–8). FFAs also activate the proinflammatory nuclear factor κB pathway (6,9), in part, via signaling through toll-like receptor-4 pathways (10). However, not all obese, insulin-resistant subjects have elevated plasma FFA levels. It is therefore likely that there are other causes for obesity-related insulin resistance. One of these appears to be endoplasmic reticulum (ER) stress. Indeed, chronic excessive nutrient intake has been shown to cause ER stress in adipose tissue of *ob/ob* mice and mice fed high-fat diets (11–13).

The ER is a major site for protein as well as for lipid and sterol synthesis (14,15). Ribosomes attached to the ER membranes release newly synthesized peptides into the ER lumen, where protein chaperones and foldases assist in the proper posttranslational modification and folding of these peptides (14–16). The properly folded proteins are then released to the Golgi complex for final modification before they are transported to their final destination. If the influx of misfolded or unfolded peptides exceeds the ER folding and/or processing capacity, ER stress ensues. Three proximal ER stress sensors have been identified. They are inositol-requiring enzyme (IRE)-1, PKR-like ER protein kinase (PERK), and activating transcription factor-6. These sensors trigger activation of pathways, termed the unfolded protein response (UPR), which act to alleviate ER stress. The UPR can achieve this by slowing protein synthesis and/or by turning up the production of protein chaperones needed for proper protein folding or, if unsuccessful, by degrading the unfolded proteins (14,16). So far, however, ER stress has only been reported in some rodent models of obesity (11–13) but not in fat of obese human subjects. We have therefore examined fat biopsy samples from lean and obese nondiabetic individuals for evidence of ER stress using proteomic, Western blot, and RT-PCR analyses.

## RESEARCH DESIGN AND METHODS

Six lean and six obese healthy volunteers were studied. Their clinical characteristics are shown in Table 1. None of the participants had a family history of diabetes or other endocrine disorders or were taking medications. Their body weights were stable for at least 2 months before the biopsies. Compared with the nonobese volunteers, the obese volunteers were heavier (93.4 vs. 77.4 kg; $P < 0.03$) and had more body fat (40.7 vs. 19.9 kg; $P = 0.004$) but had the same fat-free mass (57.6 vs. 57.6 kg) and were insulin resistant (1/homeostasis model assessment 0.44 vs. 0.29; $P < 0.05$). Informed written consent was obtained from all subjects after explanation of the nature, purpose, and potential risks of these studies. The study protocol was approved by the institutional review board of Temple University Hospital.

**Fat biopsies.** The subjects were admitted to the Temple University Hospital Clinical Research Center on the day before the studies. At ~8:00 A.M. on the

From the [1]Division of Endocrinology, Diabetes, and Metabolism and the Clinical Research Center, Temple University School of Medicine, Philadelphia, Pennsylvania; the [2]Department of Biochemistry, Temple University School of Medicine, Philadelphia, Pennsylvania; and the [3]Department of Surgery, Temple University School of Medicine, Philadelphia, Pennsylvania.
Corresponding author: Guenther Boden, bodengh@tuhs.temple.edu.
Received 5 May 2008 and accepted 13 June 2008.
Published ahead of print at http://diabetes.diabetesjournals.org on 20 June 2008. DOI: 10.2337/db08-0604.

TABLE 1
Study subjects

| | Lean | Obese | *P* |
|---|---|---|---|
| Sex (male/female) | 4/2 | 3/3 | |
| Age (years) | 36 ± 4 | 44 ± 4 | NS |
| Weight (kg) | 77.4 ± 3.4 | 93.4 ± 5.6 | 0.03 |
| Height (cm) | 180.0 ± 2.7 | 167 ± 4.5 | 0.03 |
| BMI (kg/m$^2$) | 24.0 ± 1.2 | 33.5 ± 1.6 | 0.02 |
| Fat (kg) | 19.9 ± 2.9 | 40.7 ± 5.9 | 0.004 |
| Fat-free mass (kg) | 57.6 ± 3.5 | 57.6 ± 5.7 | NS |
| 1/homeostasis model assessment | 0.441 ± 0.126 | 0.291 ± 0.02 | 0.05 |
| Fasting blood glucose (mg/dl) | 97.1 ± 2.4 | 93.5 ± 1.2 | NS |
| FFA (μmol/l) | 481 ± 81 | 424 ± 37 | NS |

Data are means ± SD.

day after admission, a venous blood sample was obtained and an open fat biopsy was performed by a surgeon. Fat biopsies were obtained from the lateral aspect of the upper thigh (~15 cm above the patella) under local anesthesia, as described (4). The excised fat was dropped immediately into isopentane and kept at its freezing point (−160°C) by liquid nitrogen. The frozen fat was stored at −80°C until analyzed.

**Sample preparation for two-dimensional gel analysis.** Frozen adipose tissue from six nonobese and six obese nondiabetic volunteers was individually processed by grinding with a mortar and pestle cooled with liquid nitrogen. Frozen powders from each individual tissue block were thawed by adding 0.8 ml of cold lysis buffer (7 mol/l urea, 2 mol/l thiourea, 4% CHAPS, 40 mmol/l Tris, and 60 mmol/l DTT) and sonicated in an ice bath for ~1 min (Sonic Dismembrator; Fisher Scientific). Sonicated solutions were centrifuged at 10,000*g* for 12 min at 4°C. Supernatants were collected and acetone added to precipitate proteins. Precipitated proteins were resolubilized using the above lysis buffer. Protein concentrations in the extracts were measured in triplicate using a Bio-Rad Bradford-based protein assay with BSA as the standard.

**Two-dimensional gel electrophoresis.** Adipose tissue lysates were processed individually (six from each group of subjects). For the first-dimension separation, 50 μg of sample protein was diluted in 125 μl of rehydration buffer and loaded onto an immobilized pH gradient (IPG) strip by overnight passive in-gel rehydration. A global view of the proteome was obtained initially using IPG strips of pI 3–10 (data not shown). To enhance resolution and sensitivity, narrow-range IPG strips (pI 4–7 and 6–10) were subsequently used. The rehydration buffer contained 8 mol/l urea, 2% CHAPS, 0.2% carrier ampholytes, and 10 mmol/l DTT for pI 4–7 linear and pI 3–10 nonlinear IPG strips. The pI 6–10 IPG strips were rehydrated with the rehydration buffer containing 15 mg/ml Destreak reagent substitute for 10 mmol/l DTT. Isoelectric focusing within the strips was performed at 20°C with a Ettan IPGphor system Amersham (Piscataway, NJ) using a total of 12,000 V/h with a maximum of 8,000 V.

For two-dimensional separation, the IPG strips were soaked for 15 min in 10 ml of equilibration buffer (6 mol/l urea, 30% glycerol, 2% SDS, 1% DTT, and 0.05 mol/l Tris, pH 8.8) followed by 15 min in 10 ml of a second equilibration buffer (with 2.5% iodoacetamide substituted for 1% DTT) and positioned against 10–14% SDS polyacrylamide gels in a Bio-Rad Mini-PROTEAN 3 System at 200 V for 45 min. Polyacrylamide gels were then fixed twice using 50% methanol, 7% acetic acid, and balance water. The resolved protein spots in the gels were visualized with Sypro-Ruby fluorescence total protein stain.

**Image analysis of two-dimensional gels.** Fluorescence images of individual gels from the 12 adipose tissue lysates were captured with a FLA-5000 Fluor Imager (Fuji Photo Film, Tokyo, Japan) and analyzed using PDQuest software (version 8.0). After automatic detection of spots by PDQuest software, the files were also inspected manually to assess accuracy of computer-generated images. The software calculated individual spot "volumes" in each gel by density/area integration. To control for slight differences in protein loading across gels, the spot volume obtained from each individual fat lysate was automatically calculated by image analysis software and normalized to total spot volume on that gel.

**In-gel trypsin digestion.** Differentially expressed spots were excised using an Xcise automated robotic system (Shimadzu Biotech, Columbia, MD). Destaining of excised gel pieces was performed by two 30-min washes with 50% acetonitrile containing 50 mmol/l ammonium bicarbonate. Following dehydration with 100% acetonitrile, 10 μl of 12.5 ng/μl sequencing grade trypsin (Promega, Madison, WI) was added to the gel pieces and incubated overnight at 37°C. Resulting tryptic peptides were extracted twice with 15 μl (5% formic acid, 50% acetonitrile, and balance water) for 20 min, and the pooled extracts were desalted with ZipTips C18 (Millipore, Billerica, MA).

**MALDI-TOF/TOF analysis.** The desalted peptides from each spot were mixed 1:1 with matrix solution (1% α-cyano-4-hydroxy cinnamic acid in 50% acetonitrile and 50% 0.1% trifluoroacetic acid), and 1.0-μl volumes were applied to wells of an AnchorChip sample target plate used for the Bruker Auto-flex MALDI-TOF/TOF instrument. Peptide mass fingerprints were obtained using the reflective and positive ion mode. Mass spectra were collected from the sum of 100–400 laser shots, and monoisotopic peaks were generated by FlexAnalysis software with signal-to-noise ratio of two to one. Mass peak value calculations used two trypsin autodigestion peptides with M + H values 842.509 and 2211.104 as internal standards. Proteins were identified by matching the calibrated peptide mass values within Swiss-Prot protein database for homosapiens using an in-house version of Mascot Server 2.1 imbedded in Bruker's Biotool software. Match variances allowed were a mass tolerance of 50 ppm, one missed trypsin cleavage, fixed modification of carbamidomethyl cysteine, and variable modification of methionine oxidation. For the samples that did not produce a "hit" with a confident score, peptide peaks with good signal were further fragmented using laser-induced decomposition to obtain LIFT-TOF/TOF spectra, and these tandem mass spectra data alone or combined with the previously produced mass spectra data were used to search against the protein database through the Mascot.

**Western blot analysis.** Proteins (30–80 μg) from the same adipose tissue lysates as used for the two-dimensional gels were separated by 10–14% gradient SDS-PAGE. The separated proteins were transferred to a nitrocellulose membrane in a semidry blotting chamber according to the manufacturer's protocol (Bio-Rad, Hercules, CA).

Blots were blocked with 5% milk in Tris-buffered saline solution (pH 7.6) containing 0.05% Tween-20 and probed with the following rabbit anti-human antibodies from Santa Cruz Biotechnology (Santa Cruz, CA) at a concentration of 0.4 μg/ml: protein disulfide isomerase A3 (PDI) (SC-20132), calreticulin (CRT) (SC-11398), and calnexin (CNX) (SC-11397). In addition, a rabbit antiserum that detects phospho c-jun $NH_2$-terminal kinase (JNK)-1, -2, and -3 (Cell Signaling Technology, Danvers, MA) and a rabbit antiserum that detects total JNK were used. Blots were incubated with primary antibody overnight at 4°C with gentle shaking and then incubated with a mouse anti-rabbit horseradish peroxidase–conjugated secondary antibody (1:10,000) (Biomeda, Foster City, CA) for 1 h at room temperature. Blots were exposed using a chemiluminescent detection method (Enhanced ECL Detection System; GE Healthcare BioSciences, Piscataway, NJ).

**RT-PCR.** Total RNAs were isolated from frozen adipose tissues, and real-time RT-PCR was performed with a SYBR Green One-Step qRT-PCR kit (Invitrogen, Carlsbad, CA) and a Light-Cycler (Roche, Indianapolis, IN). Primers for X-box binding protein (XBP)-1s (NM-005080) were sense TTGAGAACCAGGAGT TAAG and antisense CTGCACCTGCTGCGGACT.

**Statistical analysis.** Two-dimensional gel analysis was performed by PDQuest software (Bio-Rad), version 8.0. Each gel from obese and lean fat samples was enumerated and analyzed for spot detection, background subtraction, and protein spot volume quantification. Of six samples per group, the gel image showing the highest quality of spots and the best protein pattern was chosen as a reference template, and spots in a reference gel were then matched across all gels. Manual corrections were performed to validate the matches automatically generated by the software. Spot volume values were normalized in each gel by dividing the raw quantity of each spot by the total volume of all the spots included in the same gel. For each protein spot, the average spot volume values and its SD in each group were determined. The match spots were subjected to Student's *t* test in order to determine the spots that were differentially expressed. Only those spots that show a statistically significant difference with a confidence level of 0.05 were chosen for identification. To test for intergel reproducibility, two-dimensional gel analysis was performed in triplicate using one representative sample. Equal amounts of high-quality protein spots (345 for pI 4–7) were detected. The average variance (coefficient of variation) of the normalized spot volume was determined to be 19.25%.

## RESULTS

**Proteomic analysis.** Gels with isoelectric focusing ranges of PI 4–7 and 6–10 produced a total of ~900 protein spots in each gel (Fig. 1). The comparison of all spots visualized yielded 24 spots that were significantly different in lean versus obese volunteers. Three of these spots represented multiple isoforms of vimentin. Three

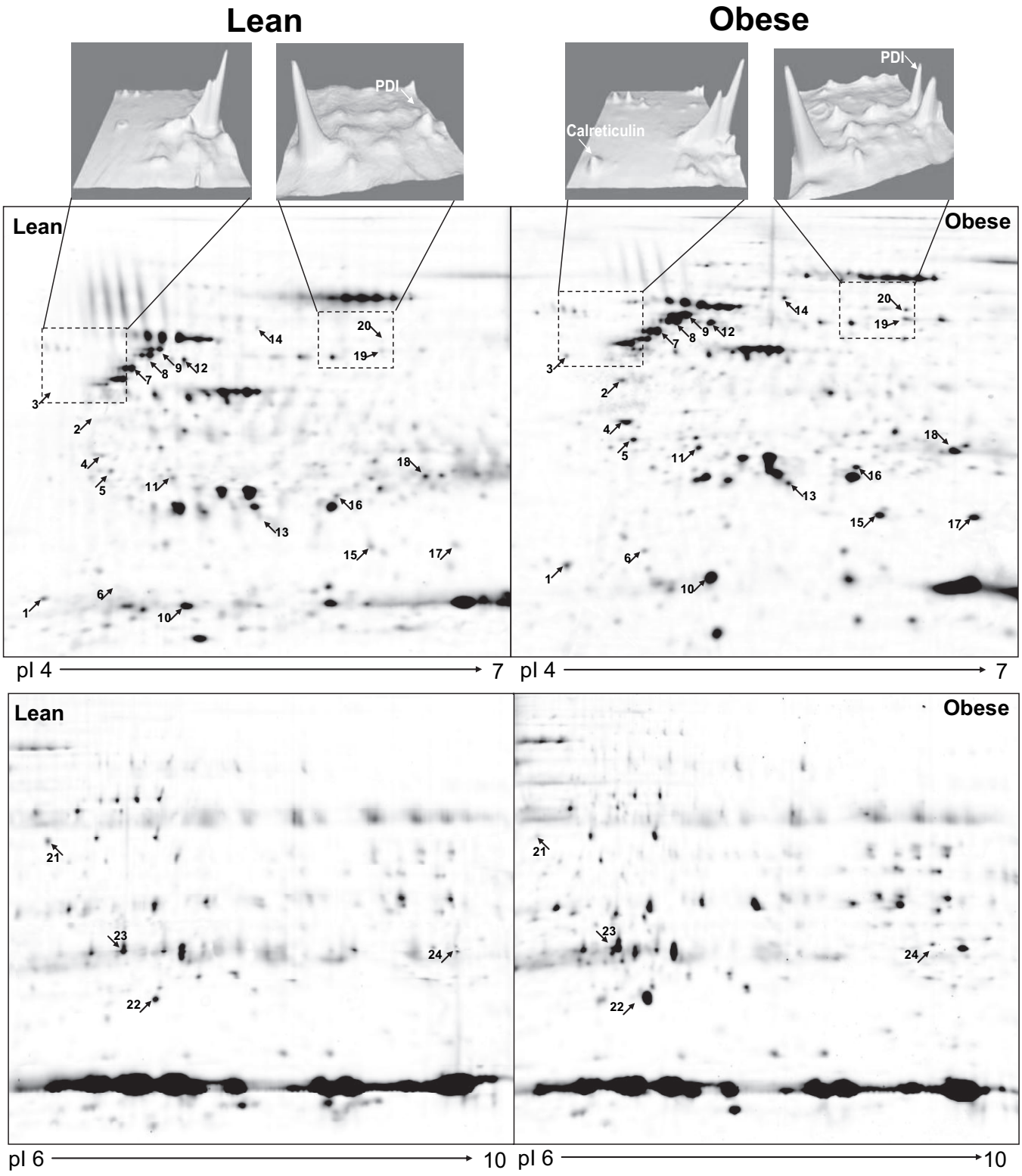


**FIG. 1. Expression levels of the UPR proteins CRT and PDI in adipose tissue of one lean and one obese subject (*upper panels*). Differentially expressed proteins in fat homogenates from one lean and one obese subject. Proteins were separated by isoelectric focusing and molecular weight (2-DG) as described in RESEARCH DESIGN AND METHODS. The subproteom from each sample was assessed using Pi ranges of 4–7 (*middle panels*) and 6–10 (*lower panels*). The proteins were stained with spyro-ruby and images compared by PD Quest software. The numbers correspond to the spot numbers in Table 2. The arrows indicate upregulated proteins in the fat of obese subjects.**

vimentin isoforms were considered as one protein (24 − 2 = 22). Two other spots could not be identified (22 − 2 = 20). Of 20 remaining differentially expressed proteins, 19 were upregulated and 1 (α-enolase) was downregulated in obese versus lean volunteers (Table 2). The differentially expressed proteins were grouped into the following categories: *1*) UPR and stress (seven proteins), *2*) energy and FFA metabolism (five proteins), *3*) structural proteins (four proteins), and *4*) protein transport and signaling (four proteins) (Table 2).

TABLE 2
Proteins differentially expressed in two-dimensional gels

| Spot no. | Protein identification | Swiss protein accession no. | Mouse score | Peptides matched | Normalized spot volumes ± SD (lean; $n = 6$) | Normalized spot volumes ± SD (obese; $n = 6$) | $P$ |
|---|---|---|---|---|---|---|---|
| UPR and stress | | | | | | | |
| 3 | CRT | P27797 | 66 | 7 | 0 | 1,019 ± 236 | <0.001 |
| 23 | PDI | P30101 | 61 | 6 | 421 ± 328 | 1,170 ± 63 | <0.01 |
| 20 | 20 kDa HSPβ-6 | 014558 | 76 | 5 | 2,534 ± 1,157 | 7,530 ± 248 | 0.001 |
| 21 | 27 kDa HSPβ-1 | P04792 | 78 | 8 | 4,242 ± 1,438 | 8,140 ± 1643 | 0.001 |
| 25 | HSPβ-5 | P02511 | 74 | 9 | 4,162 ± 558 | 8,967 ± 2,918 | 0.049 |
| 16 | 60 kDA HSP | P10809 | 69 | 6 | 600 ± 558 | 1,868 ± 56 | <0.001 |
| 19 | Glutathione-*S*-transferase P | P09211 | 107 | 8 | 2,231 ± 698 | 3,936 ± 390 | 0.013 |
| Energy and FFA metabolism | | | | | | | |
| 12 | ATP synthase subunit-β | P06576 | 138 | 11 | 2,413 ± 801 | 5,499 ± 1,251 | 0.01 |
| 15 | Perilipin | 060240 | 57 | 6 | 1,602 ± 381 | 3,960 ± 1,019 | 0.007 |
| 22 | Aldehyde dehydrogenase | P05091 | 87 | 9 | 1,341 ± 161 | 4,088 ± 799 | 0.001 |
| 24 | α-Enolase | P06733 | 65 | 7 | 803 ± 214 | 293 ± 74 | 0.018 |
| 26 | Carbonic anhydrase-1 | P00915 | 108 | 11 | 2,463 ± 774 | 4,846 ± 523 | 0.012 |
| Structural proteins | | | | | | | |
| 1 | Myosin light-chain polypeptide-6 | P60660 | 60 | 6 | 1,792 ± 528 | 3,837 ± 284 | 0.002 |
| 2 | Tropomyosin β-chain | P07951 | 58 | 6 | 1,141 ± 443 | 4,072 ± 531 | 0.03 |
| 4 | Tropomyosin α4-chain | P67936 | 94 | 8 | 770 ± 355 | 3,429 ± 779 | 0.002 |
| 7–9 | Vimentin | P08670 | 204 | 19 | 3,136 ± 1,418 | 11,005 ± 3,353 | 0.007 |
| Protein transport and signaling | | | | | | | |
| 6 | γ-Synuclein | 076070 | 66 | 4 | 488 ± 465 | 1,714 ± 670 | 0.034 |
| 11 | ρGDP dissociation inhibitor-1 | P52565 | 75 | 5 | 2163 ± 612 | 3,168 ± 286 | 0.049 |
| 5 | 14-3-3 protein-γ | P61981 | 78 | 6 | 875 ± 525 | 3,619 ± 1,005 | 0.005 |
| 10 | Galectin-1 | P09382 | 113 | 10 | 9,030 ± 1,387 | 25,049 ± 4,175 | 0.001 |

Data are means ± SD.

**UPR and stress.** Levels of expression of the following UPR proteins were overexpressed in two-dimensional gels in adipose tissue from obese volunteers: CRT, a protein chaperone, increased from undetectable to 1,019 ± 236 arbitrary units; PDI, a protein foldase, increased approximately threefold; and glutathione-*S*-transferase P, an antioxidant protein belonging to a UPR-regulated pathway, increased ~1.8-fold (Fig. 1; Table 2).

Several cytosolic small heat shock proteins (HSPs) (20 and 27 kDa HSP) and one mitochondrial HSP (60 kDa HSP) were also overexpressed in the adipose tissue of obese volunteers, suggesting the presence of cytosolic and mitochondrial stress in addition to ER stress (Table 2).

**Other proteins.** Several proteins involved in energy and FFA metabolism (ATP synthase subunit-β, perilipin, aldehyde dehydrogenase, α-enolase, and carbonic anhydrase-1), structural proteins (myosin light-chain polypeptide-6, tropomyosin β-chain, tropomyosin α4-chain, and vimentin), and proteins involved in transport and signaling (γ-synuclein, ρ-guanosine 5′-diphosphate dissociation inhibitor-1, 14-3-3 protein-γ, and galectin-1) were also differentially overexpressed in fat from obese volunteers (Table 2).

**Western blot analysis.** Western blotting confirmed upregulation of CRT and PDI and revealed upregulation of CNX (~1.8-fold), a membrane bound chaperone and phospho-JNK-1 ~2.0-fold, a downstream effector protein of the UPR. Phospho-JNK 2/3, however was unchanged (Fig. 2).

**RT-PCR analysis.** Upregulation of the spliced form of XBP-1s, a part of the IRE-1/XBP-1 proximal ER stress sensor, and of tumor necrosis factor-α, a proinflammatory cytokine, were documented with RT-PCR, whereas there were no differences in interleukin-1β and -6 mRNA in adipose tissue of lean and obese subjects (Fig. 3).

## DISCUSSION

In the present study, we found activation of one of three UPR proteins, known to be proximal ER stress sensors (IRE-1/XBP-1), but failed to detect statistically significant activation of the other two ER stress sensors (activating transcription factor-6 and PKR-like ER protein kinase) and two other UPR proteins (glucagon-like peptide-78 and C/EBP homologous protein) in fat from obese subjects (data not shown). This

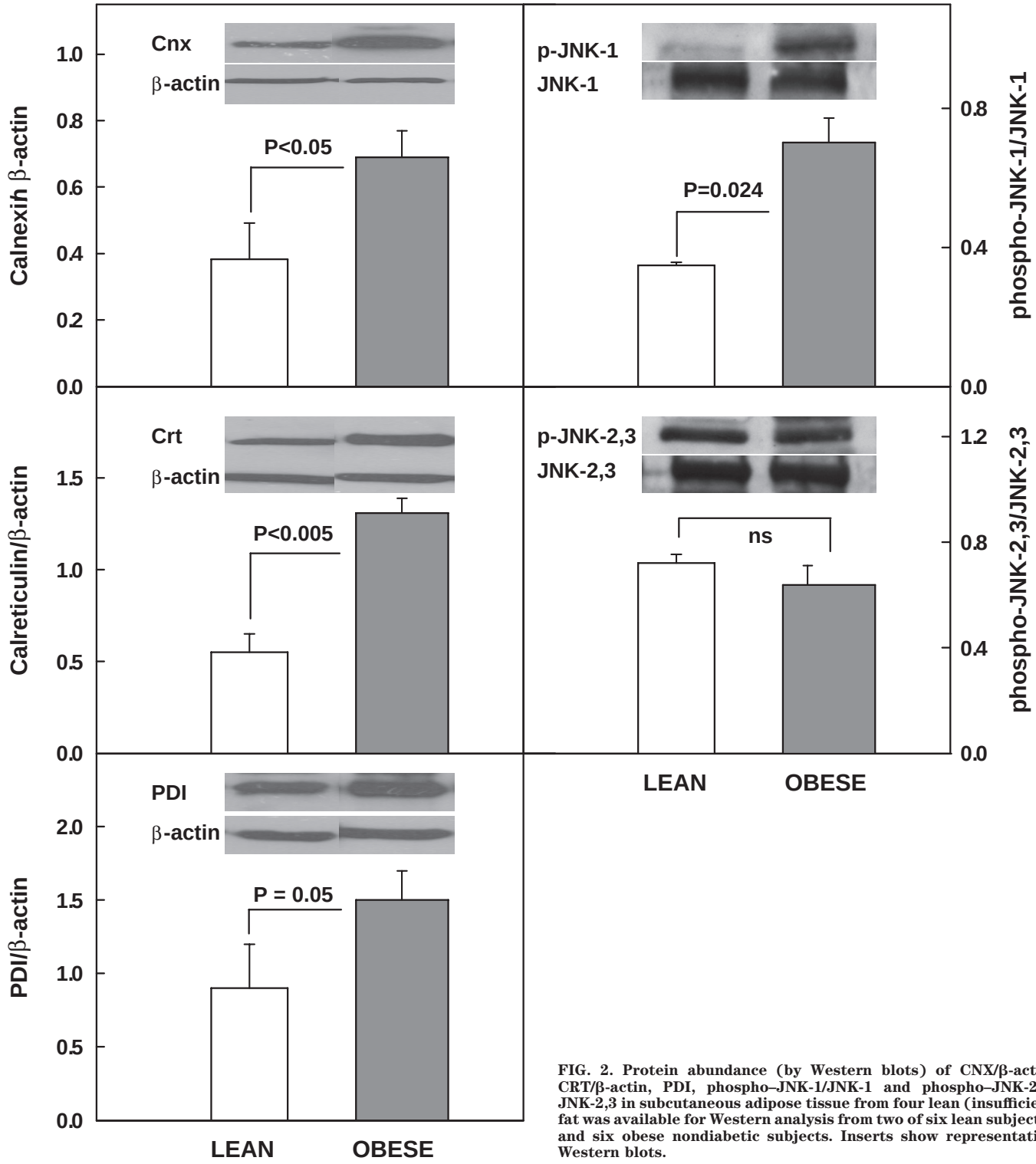


**FIG. 2. Protein abundance (by Western blots) of CNX/β-actin, CRT/β-actin, PDI, phospho–JNK-1/JNK-1 and phospho–JNK-2,3/JNK-2,3 in subcutaneous adipose tissue from four lean (insufficient fat was available for Western analysis from two of six lean subjects) and six obese nondiabetic subjects. Inserts show representative Western blots.**

was not surprising, as it has previously been shown that only severe and long-lasting ER stress activates all three UPR pathways simultaneously, whereas different duration and types of ER stress can activate one, two, or all three pathways in different tissues (17).

The IRE-1/XBP-1 pathway regulates induction of chaperone synthesis. IRE-1 activation results in dimerization and autophosphorylation of IRE-1. This activates IRE-1's endonuclease activity and initiates splicing of a 26-bp segment from the XBP-1 mRNA, creating XBP-1s, a potent transcription factor that targets genes encoding ER chaperones, including CRT, CNX, and PDI, a foldase that catalyzed disulfide bond formation (14,17,18). XBP-1s mRNA, CRT, CNX, and PDI were all upregulated in fat of obese compared with nonobese volunteers (Figs. 1–3), indicating activation of UPR and suggesting presence of ER stress. The lectin/chaperones CNX and CRT facilitate protein folding by shielding unfolded protein regions from surrounding proteins, thus preventing aggregation. In addition, the CNX/CRT cycle is one arm of the quality-control machinery in the ER that monitors the glyco-

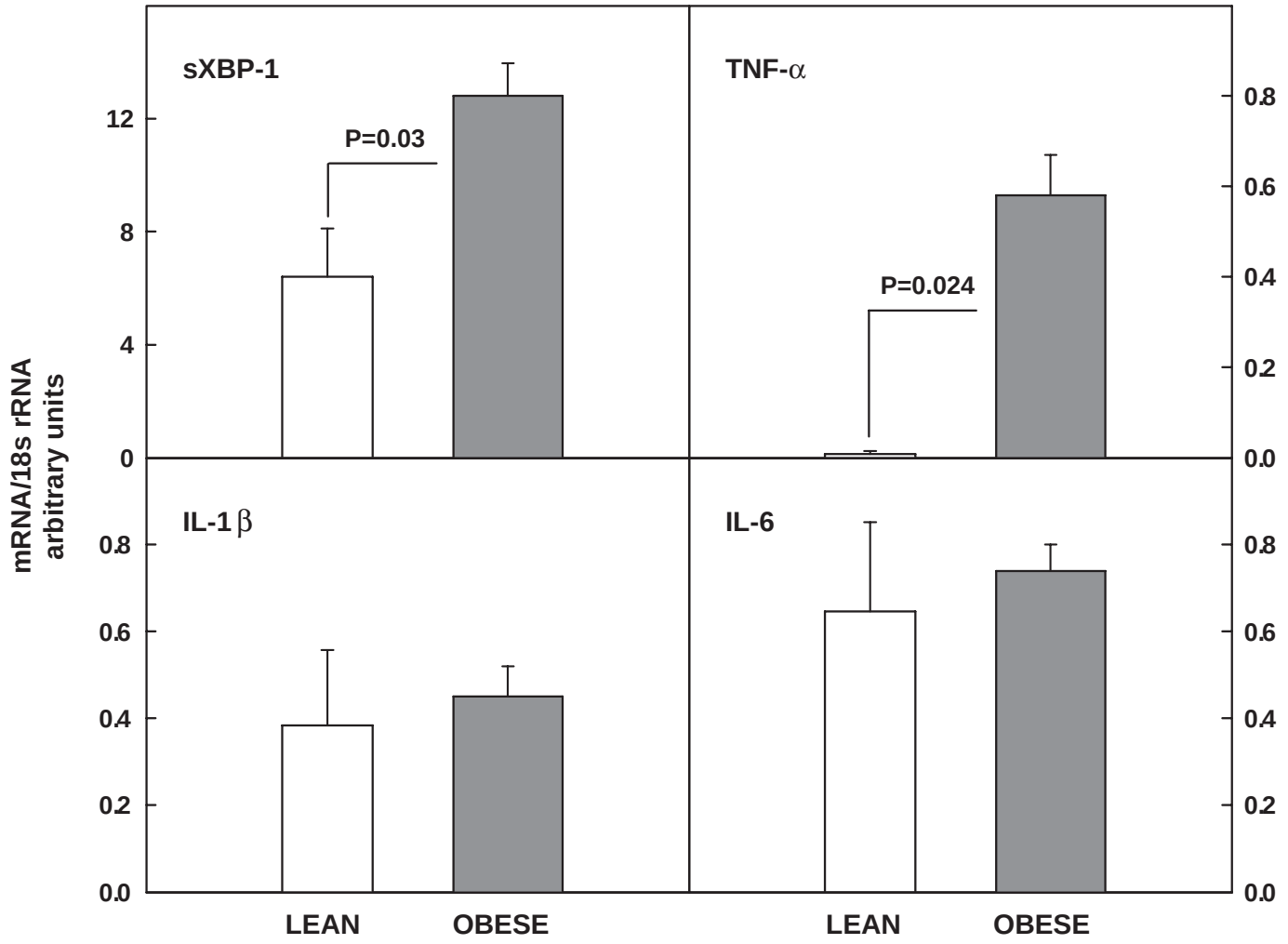


**FIG. 3. Messenger RNA (mRNA) corrected for 18s ribosomal RNA (18sr RNA) of sXBP-1, tumor necrosis factor-α, interleukin-1β, and interleukin-6 in six lean and six obese nondiabetic subjects.**

sylation status of proteins and determines whether a molecule is exported to the Golgi complex or targeted for ER-associated degradation (14,19).

In addition, we found phospho–JNK-1 (but not phospho–JNK-2 or phospho–JNK-3) to be markedly upregulated. ER stress has previously been reported to activate JNK to phospho-JNK (primarily to phospho–JNK-1) in cultured cells and animal models (11,20–22). JNK activation is coupled to ER stress–induced IRE-1 activation through recruitment of tumor necrosis factor receptor–associated factor-2 and apotosis signal–regulating kinase-1 to the cytosolic leaflet of the ER membrane (22). The complex of these three proteins phosphorylates and activates JNK. JNK activation has been shown to produce insulin resistance and inflammation, while JNK inhibition improved insulin sensitivity in fat, liver, and muscle of several animal models of obesity (11).

Proteosome analysis also revealed a 3.5-fold increase in γ-synuclein. γ-Synuclein belongs to a family of small unfolded proteins with unknown physiological functions. γ-Synuclein has been detected in various cancers, particularly in advanced stages of breast and ovarian cancer (23). In vitro, γ-synuclein inhibits normal metastatic checkpoint control, promotes cancer invasion and metastasis, and is being used as a marker for assessing breast cancer progression (24). The observed large upregulation of γ-synuclein in fat from obese individuals is interesting in view of the recognized increase in cancer risk in obesity (25,26).

Pertubation of ER function was not restricted to the ER but involved other sections of the protein secretory pathway, as indicated by upregulation of several cytosolic protein chaperones including three small HSPs (20 kDa HSPβ-6, 27 kDa HSPβ-1, and HSPβ-5). In addition, it involved mitochondria, as evidenced by upregulation of the mitochondrial 60-kDa HSP (chaperonin), which participates in the folding of newly synthesized proteins that are transported from the cytosol to mitochrondria (14).

White adipose tissue hypoxia associated with increased expression of ER stress markers has been reported in mice (27,28). To explore a possible role of adipose tissue hypoxia in the observed UPR, we have determined expression of hemoxygenase-1 (hemox-1). This gene has been shown to be dramatically upregulated in fat of hypoxic *ob/ob* mice (28). There was, however, no difference in the hemoxygenase-1 mRNA/18 small-subunit ribosomal RNA ratios in subcutaneous fat from lean and obese subjects (0.5 vs. 0.5; $P$ = NS).

It has been shown, in vitro and in animal models, that nutrient excess (the cause for obesity) produces ER stress (11,12), and it has been speculated that the reason for ER stress in response to nutrient excess may be increased demand for lipid and protein synthesis and for structural

changes in the organs primarily involved in metabolizing and storing excess nutrients (i.e., the adipose tissue and the liver) (12). Compatible with this interpretation, we found overexpression of several structural proteins and proteins related to energy and fat metabolism and protein transport. Moreover, an increase in reactive oxygen species (ROS), which frequently accompanies nutrient excess, can cause ER stress (29) and activate the UPR (30).

ER stress has been demonstrated to trigger activation of several serine/threonine kinases, including JNK and IκB kinase and is a major source for the production of ROS, which not only produces insulin resistance but also stimulates synthesis and release of proinflammatory cytokines and chemokines such as tumor necrosis factor-α, interleukin-1β, interleukin-6, and monocyte chemotactic protein-1 (11 and this article). Thus, the ER might be a proximal site that senses nutritional excess and translates that excess into metabolic and inflammatory responses (12). Finally, all our fat biopsies were from thigh subcutaneous adipose tissue, and, thus, the results may not be representative of fat in other locations.

## ACKNOWLEDGMENTS

This work was supported by National Institutes of Health grants R01-DK58895, HL-0733267, and R01-DK066003 (all to G.B.); a grant from the Groff Foundation; a Mentor-Based Training Grant from the American Diabetes Association (to G.B.); and R01-A1064017 (to S.M.).

We thank Constance Harris Crews for typing the manuscript and Maria Mozzoli for technical assistance.

## REFERENCES

1. Bray GA: Medical consequences of obesity. *J Clin Endocrinol Metab* 89:2583–2589, 2004
2. Boden G: Obesity, insulin resistance, type 2 diabetes and free fatty acids. *Expert Rev Endocrinol Metab* 1:499–505, 2006
3. Reaven GM, Hollenbeck C, Jeng C-Y, Wu MS, Chen YD: Measurement of plasma glucose, free fatty acid, lactate and insulin for 24 h in patients with NIDDM. *Diabetes* 37:1020–1024, 1988
4. Boden G, Chen X, Ruiz J, White JV, Rossetti L: Mechanisms of fatty acid-induced inhibition of glucose uptake. *J Clin Invest* 93:2438–2446, 1994
5. Santomauro AT, Boden G, Silva M, Rocha DM, Santos RF, Ursich MJ, Strassmann PG, Wajchenberg BL: Overnight lowering of free fatty acids with acipimox improves insulin resistance and glucose tolerance in obese diabetic and nondiabetic subjects. *Diabetes* 48:1836–1841, 1999
6. Itani SI, Ruderman NB, Schmieder F, Boden G: Lipid-induced insulin resistance in human muscle is associated with changes in diacylglycerol, protein kinase C, and IκB-α. *Diabetes* 51:2005–2011, 2001
7. Neschen S, Morino K, Hammond LE, Zhang D, Liu ZX, Romanelli AJ, Cline GW, Pongratz RL, Zhang MX, Choi CS, Coleman RA, Shulman GI: Prevention of hepatic steatosis and hepatic insulin resistance in mitochondrial acyl-CoA:glycerol-sn-3-phosphate acyltransferase 1 knockout mice. *Cell Metab* 2:55–65, 2005
8. Yu C, Chen Y, Cline GW, Zhang D, Zong H, Wang Y, Bergeron R, Kim JK, Cushman SW, Cooney GJ, Atcheson B, White MF, Kraegen EW, Shulman GI: Mechanism by which fatty acids inhibit insulin activation of insulin receptor substrate-1 (IRS-1)-associated phosphatidylinositol 3-kinase activity in muscle. *J Biol Chem* 277:50230–50236, 2002
9. Boden G, She P, Mozzoli M, Cheung P, Gumireddy K, Reddy P, Xiang X, Luo Z, Ruderman N: Free fatty acids produce insulin resistance and activate the proinflammatory nuclear factor-κB pathway in rat liver. *Diabetes* 54:3458–3465, 2005
10. Shi H, Kokoeva MV, Inouye K, Tzameli I, Yin H, Flier JS: TLR4 links innate immunity and fatty acid-induced insulin resistance. *J Clin Invest* 116:3015–3025, 2006
11. Hirosumi J, Tuncman G, Chang L, Gorgun CZ, Uysal KT, Maeda K, Karin M, Hotamisligil GS: A central role for JNK in obesity and insulin resistance. *Nature* 420:333–336, 2002
12. Ozcan U, Cao Q, Yilmaz E, Lee A-H, Iwakoshi NN, Ozdelen E, Tuncman G, Gorgun C, Glimcher LH, Hotamisligil GS: Endoplasmic reticulum stress links obesity, insulin action, and type 2 diabetes. *Science* 306:457–461, 2004
13. Nakatani Y, Kaneto H, Kawamori D, Yoshiuchi K, Hatazaki M, Matsuoka TA, Ozawa K, Ogawa S, Hori M, Yamasaki Y, Matsuhisa M: Involvement of endoplasmic reticulum stress in insulin resistance and diabetes. *J Biol Chem* 280:847–851, 2005
14. Schroder M, Kaufman RJ: The mammalian unfolded protein response. *Annu Rev Biochem* 74:739–789, 2005
15. Wang H, Kouri G, Wollheim CB: ER stress and SREBP-1 activation are implicated in β-cell glucolipotoxicity. *J Cell Sci* 118:3905–3915, 2005
16. Gregor MF, Hotamisligil GS: Adipocyte stress: the endoplasmic reticulum and metabolic disease. *J Lipid Res* 48:1905–1914, 2007
17. Wu J, Kaufman RJ: From acute ER stress to physiological roles of the unfolded protein response. *Cell Death Differ* 13:374–384, 2006
18. Calfon M, Zeng H, Urano F, Till JH, Hubbard SR, Harding HP, Clark SG, Ron D: IRE1 couples endoplasmic reticulum load to secretory capacity by processing the XBP-1 mRNA. *Nature* 415:92–96, 2002
19. Trombetta ES, Helenius A: Conformational requirements for glycoprotein reglucosylation in the endoplasmic reticulum. *J Cell Biol* 148:1123–1129, 2000
20. Kyriakis M, Banerjee P, Nikolakaki E, Dai T, Ruble EA, Ahmad MF, Avruch J, Woodgett JR: The stress-activated protein kinase subfamily of c-Jun kinases. *Nature* 369:156–160, 1994
21. Srivastava RK, Sollott SJ, Khan L, Hansford R, Lakatta EG, Longo DL: Bcl-2 and Bcl-X(L) thapsigargin-induced nitric oxide generation, c-Jun $NH_2$-terminal kinase activity, and apoptosis. *Mol Cell Biol* 19:5659–5674, 1999
22. Urano F, Wang X, Bertolotti A, Zhang Y, Chung P, Harding HP, Ron D: Coupling stress in the ER to activation of JNK protein kinases by transmembrane protein kinase IRE 1. *Science* 287:664–666, 2000
23. Ahmad M, Attoub S, Singh MN, Martin FL, El-Agnaf OMA: γ-Synuclein and the progression of cancer. *FASEB J Rev* 21:3419–3430, 2007
24. Wu K, Quan Z, Weng Z, Li F, Zhang Y, Yao X, Chen Y, Budman D, Goldberg ID, Shi YE: Expression of neuronal protein synuclein gamma gene as a novel marker for breast cancer prognosis. *Breast Cancer Res Treat* 101:259–267, 2006
25. Lew EA, Garfinkel L: Variations in mortality by weight among 750,000 men and women. *J Chronic Dis* 32:563–576, 1979
26. Manson JE, Willett WC, Stampfer MJ, Colditz GA, Hunger DJ, Hankinson SE, Hennekens CH, Speizer FE: Body weight and mortality among women. *N Engl J Med* 333:677–685, 1995
27. Hosogai N, Fukuhara A, Oshima K, Miyata Y, Tanaka S, Segawa K, Furukawa S, Tochino Y, Komuro R, Matsuda M, Shimomura I: Adipose tissue hypoxia in obesity and its impact on adipocytokine dysregulation. *Diabetes* 56:901–911, 2007
28. Ye J, Gao Z, Yin J, He Q: Hypoxia is a potential risk factor for chronic inflammation and adiponectin reduction in adipose tissue of ob/ob and dietary obese mice. *Am J Physiol Endocrinol Metab* 293:E1118–E1128, 2007
29. Furukawa S, Fujita T, Shimabukuro M, Iwaki M, Yamada Y, Nakajima Y, Nakayama O, Makishima M, Matsuda M, Shimomura I: Increased oxidative stress in obesity and its impact on metabolic syndrome. *J Clin Invest* 114:1752–1761, 2004
30. Xue X, Piao J-H, Nakajima A, Sakon-Komazawa S, Kojima Y, Mori K, Yagita H, Okumura K, Harding H, Nakano H: Tumor necrosis factor alpha (TNF-α) induces the unfolded protein response (UPR) in a reactive oxygen species (ROS)-dependent fashion, and the UPR counteracts ROS accumulation by TNF-α. *J Biol Chem* 280:33917–33925, 2005